2013

Cholera Toxin Activates The Unfolded Protein Response Through An Adenylate Cyclase-independent Mechanism

Neyda VanBennekom
University of Central Florida

CHOLERA TOXIN ACTIVATES THE UNFOLDED PROTEIN RESPONSE THROUGH AN ADENYLATE CYCLASE-INDEPENDENT MECHANISM

by

NEYDA VANBENNEKOM
B.S. University of Central Florida, 2011

A dissertation submitted in partial fulfillment of the requirements
for the degree of Master of Science
in the Department of Biomedical Sciences
in the College of Medicine
at the University of Central Florida
Orlando, Florida

Summer Term
2013

Major Professor: Kenneth Teter

ABSTRACT

Cholera toxin (CT) is a bacterial protein toxin responsible for the gastrointestinal disease known as cholera. CT stimulates its own entry into intestinal cells after binding to cell surface receptors. Once internalized, CT is delivered via vesicle-mediated transport to the endoplasmic reticulum (ER), where the CTA1 subunit dissociates from the rest of the toxin and is exported (or translocated) into the cytosol. CTA1 translocates from the ER lumen into the host cytosol by exploiting a host quality control mechanism called ER-associated degradation (ERAD) that facilitates the translocation of misfolded proteins into the cytosol for degradation. Cytosolic CTA1, however, escapes this fate and is then free to activate its target, heterotrimeric G-protein subunit alpha (Gsα), leading to adenlyate cyclase (AC) hyperactivation and increased cAMP concentrations. This causes the secretion of chloride ions and water into the intestinal lumen. The result is severe diarrhea and dehydration which are the major symptoms of cholera.

CTA1's ability to exploit vesicle-mediated transport and ERAD for cytosolic entry demonstrates a potential link between cholera intoxication and a separate quality control mechanism called the unfolded protein response (UPR), which up-regulates vesicle-mediated transport and ERAD during ER stress. Other toxins in the same family such as ricin and Shiga toxin were shown to regulate the UPR, resulting in enhanced intoxication.

Here, we show UPR activation by CT, which coincides with a marked increase in cytosolic CTA1 after 4 hours of toxin exposure. Drug induced-UPR activation also increases CTA1 delivery to the cytosol and increases cAMP concentrations during intoxication. We investigated whether CT stimulated UPR activation through Gsα or AC. Chemical activation of Gsα induced the UPR and increased CTA1 delivery to the cytosol. However, AC activation did

not increase cytosolic CTA1 nor did it activate the UPR. These data provide further insight into the molecular mechanisms that cause cholera intoxication and suggest a novel role for Gsα during intoxication, which is UPR activation via an AC-independent mechanism.

I dedicate this work to my family which I am so lucky to have in my life. Dad, Dave, Albert, and Sabia, thank you for your continued support. Mom and Cinthya, thank you for the reassurance and for believing in me. To the love of my life, Chris, thank you for listening to the words "cholera toxin" a million times, for being the magnanimous character that you are, and for sharing this journey called life with me. Words really cannot express what you all mean to me and how much your never-ending love has shaped the person that I am today.

ACKNOWLEDGMENTS

I would like to thank Drs. William Self, Scott Mills, Ron Prywes, and Mike Jobling for providing sodium selenite, CHO-β_2AR cells, luciferase reporter constructs, and mutant toxins respectively. My committee deserves thanks for their helpful input during discussions. Dr. Kim Schneider, thank you for your support. Thanks should also go to my lab mates: I would never have found anything in the lab without you. Thanks to Dr. Tuhina Banerjee for assisting with protocols. Dr. Mike Taylor, thank you for your continued patience while teaching me how to analyze SPR data. Dr. Ken Teter, I am grateful that you are my mentor, and a super awesome one at that. Thank you for your guidance, encouragement, and for inspiring the next generation of scientists.

TABLE OF CONTENTS

LIST OF FIGURES

LIST OF ACRONYMS/ABBREVIATIONS

AC	adenylate cyclase
ARF6	ADP-ribosylating factor 6
ATF6	activating transcription factor 6
β_2AR	beta-2 adrenergic receptor
BfA	brefeldin A
cAMP	cyclic adenosine monophosphate
CT	cholera toxin
DMEM	Dulbecco's modified Eagle's medium
EDC	1-ethyl-3-(3-dimethyl aminopropyl) carbodiimide
ER	endoplasmic reticulum
ERAD	endoplasmic reticulum-associated degradation
FBS	fetal bovine serum
For	forskolin
GM1	monosialotetrahexosylganglioside
Gsα	heterotrimeric G protein subunit alpha
Hsp90	heat shock protein 90
Iso	isoproterenol
IRE1	inositol-requiring enzyme 1
k_a	association rate constant
mt	mutant

NHS	*N*-hydroxysuccinimide
PBS	phosphate buffered saline
PBST	phosphate buffered saline with Tween 20
PERK	protein kinase RNA-like endoplasmic reticulum kinase
PDI	protein disulfide isomerase
SDS-PAGE	sodium dodecyl sulfate polyacrylamide gel electrophoresis
TBST	tris-buffered saline with Tween 20
Tm	tunicamycin
Tg	thapsigargin
UPR	unfolded protein response
UPRE	unfolded protein response element
wt	wild-type
XBP1	x-box binding protein 1

CHAPTER ONE: INTRODUCTION

Overview

Cholera is an intestinal infection that is endemic in many countries worldwide and affects millions of people each year (1, 2). Cholera is caused by the ingestion of the bacterium *Vibrio cholerae* in contaminated food or water. Once inside the host intestine, *V. cholerae* secretes a major virulence factor known as cholera toxin (CT), leading to symptoms including massive diarrhea and dehydration which can lead to death if left untreated (3, 4).

CT is classified as a binary AB toxin because it is composed of two major subunits: an enzymatic A subunit (CTA1) and a B subunit (CTB) responsible for cell binding (5, 6). CTB can bind to the GM1 host cell receptor on intestinal cells, stimulating toxin entry into cells by internalization into endosomes (7, 8). CT is then delivered by vesicle-mediated transport from the endosome to the endoplasmic reticulum (ER), where the CTA1 subunit can dissociate from the rest of the toxin (9, 10). Dissociated CTA1 in the ER lumen is in an unfolded state which leads to its exportation (i.e. translocation) from the ER lumen into the cytosol through a protein channel in the ER membrane (11).

Cytosolic CTA1 regains its conformation, associates with ADP-ribosylating factor 6 (ARF6), and is then free to carry out its enzymatic function (12-14) which is to modify Gsα (the stimulatory subunit of heterotrimeric G protein) by ADP-ribosylation (15, 16). This modification locks Gsα in an on state, leading to adenlyate cyclase (AC) hyperactivation, increased cAMP concentrations, and ultimately the secretion of chloride ions into the lumen of the intestines. This osmotic imbalance in turn causes the secretion of water into the intestinal lumen which results in the severe diarrhea and dehydration associated with the symptoms of cholera (1, 3, 17). Cholera

intoxication is a general term used to describe the overall mechanism of CT entry and activity within cells (Figure 1). Intoxication of tissue culture cells can be assessed by the levels of CTA1 within the cytosol as well as cellular cAMP concentrations.

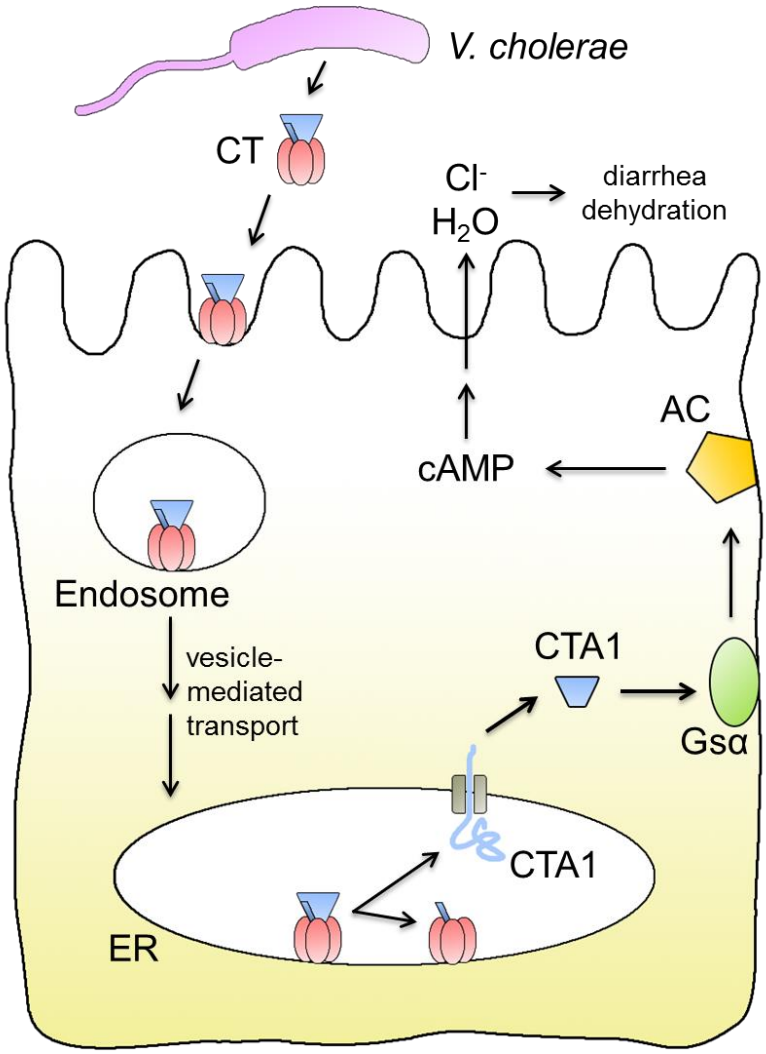

Figure 1: Mechanism of cholera intoxication

After binding to GM1, CT enters the cell and is delivered via vesicle-mediated transport to the ER, where the CTA1 subunit dissociates and is translocated into the cytosol. Cytosolic CTA1 then activates Gsα, leading to AC hyperactivation and increased cAMP concentrations. This causes the secretion of chloride ions and water into the intestinal lumen. The result is severe diarrhea and dehydration which are the major symptoms of cholera.

Translocation of CT and other AB toxins into the host cytosol

Since Gsα is located at the cytosolic face of the plasma membrane, CTA1 has to cross the ER membrane barrier in order to enter the cytosol and cause intoxication (18). CTA1 translocation occurs due to a series of events including internalization, vesicle-mediated transport through various cellular compartments, and the ability of CTA1 to exploit an ER homeostasis mechanism called the ER-associated degradation (ERAD) pathway (19-21). ERAD normally facilitates the translocation of misfolded proteins of host origin from the ER into the cytosol for degradation by the proteasome (9). As dissociated CTA1 within the ER is in an unfolded state, CTA1 can exploit ERAD for entry into the cytosol; however, it escapes the degradative fate of ERAD by assuming a stable conformation in the cytosol and is then able to modify Gsα (19, 21). Other AB toxins utilize a similar route for cytosolic entry. Ricin and Shiga toxin are thought to use ERAD to translocate from the ER into the cytosol, where the toxins modify 28S rRNA to inhibit protein synthesis and cause cell death (9, 19, 22, 23). Other AB toxins do not utilize ERAD because they cross the membrane barrier directly through the endosome (24). After toxin internalization into the endosome, the B subunit of these toxins form a pore in the endosome membrane, facilitating translocation of the enzymatic A subunit into the cytosol.

ERAD, ER stress, and the unfolded protein response

When ERAD is not able to deal with the amount of misfolded proteins within the ER, a condition known as ER stress occurs. A separate host stress response system called the unfolded protein response (UPR) is then induced. The UPR functions to reduce ER stress and does so through a variety of mechanisms (25). The PERK pathway of the UPR downregulates overall

protein synthesis in order to reduce the accumulation of proteins within the ER. Although overall protein synthesis is decreased, a select subset of proteins is upregulated through the ATF6 and IRE1 pathways to help reduce ER stress. Such proteins include chaperones to help misfolded proteins achieve a stable conformation as well as proteins involved in the ERAD pathway and vesicle-mediated transport (26, 27) to help clear the ER of proteins. The upregulation of ERAD and vesicle trafficking proteins during the UPR and the ability of CTA1 to exploit these same host processes for translocation demonstrates a potential link between cholera intoxication and the UPR.

The ability of AB toxins to regulate the UPR and enhance intoxication

Other AB toxins, such as ricin and Shiga toxin, have been shown to regulate the UPR resulting in enhanced intoxication (28-31). Ricin is able to inhibit the IRE1 and PERK pathways of the UPR in yeast (29) and mammalian cells (31) which enhances cytotoxicity (29). However, a conflicting study found that ricin induces the PERK and ATF6 pathways of the UPR in mammalian cells (30). Shiga toxin has been shown to induce all three pathways of the UPR to enhance cell death during intoxication (28).

Although the UPR is regulated by Shiga toxin and ricin, the same has not been established for CT. However, there is evidence to suggest that UPR activation may enhance intoxication as it does for ricin and Shiga toxin. A study published in 1996 showed that treatment with thapsigargin, a chemical now known to induce the UPR, increased CT transport and cAMP concentrations during intoxication (32). Thapsigargin depletes the ER calcium stores, inhibiting the function of calcium-dependent chaperones within the ER which causes an increase in

misfolded proteins and activation of the UPR (33). The study focused on the effect of calcium concentrations on intoxication rather than the effect of the UPR on intoxication as the UPR was not well understood at the time.

We predict that CT may promote delivery of CTA1 molecules to the cytosol by inducing the UPR, exploiting the effects of the UPR such as increased activity in ERAD or vesicle-mediated transport. This activation could lead to enhanced intoxication measured by increased levels of cytosolic CTA1 and increased concentrations of cAMP (Figure 2).

This work elucidates whether CT is able to exploit another host process, the unfolded protein response, in order to cause enhance intoxication. If the UPR is induced by CT, as it is for the aforementioned AB toxins, then the project will also establish novel roles for CT and/or for host factors that act downstream of CT during toxin-induced UPR activation.

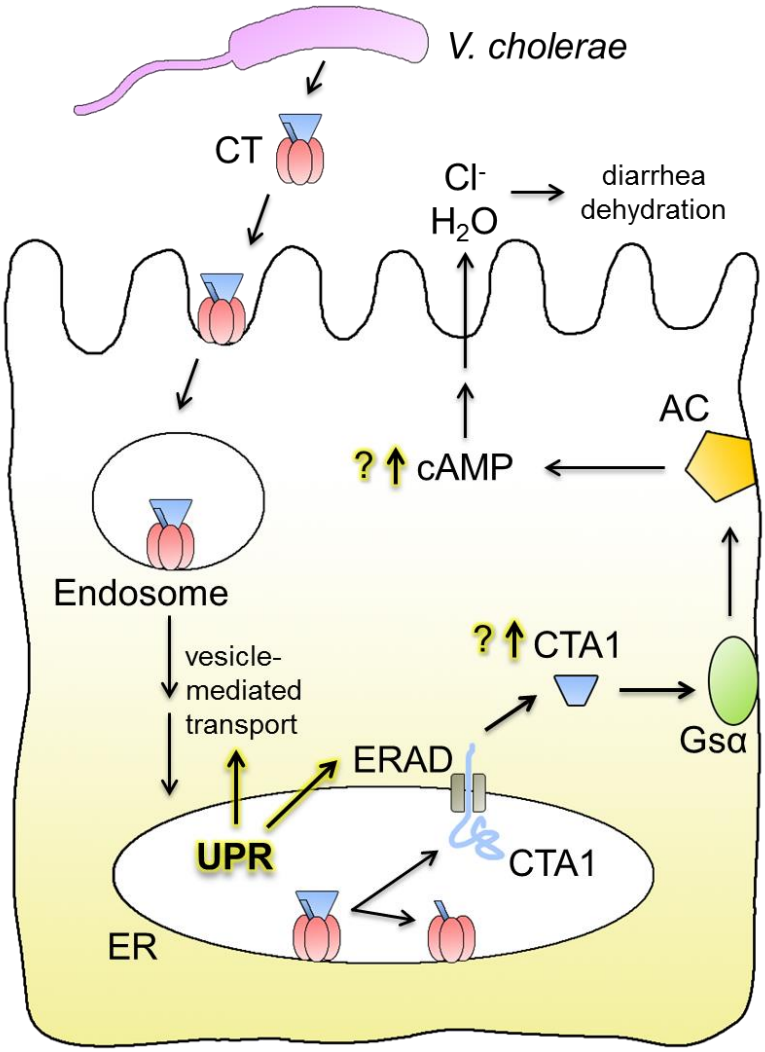

Figure 2: Potential effects of an UPR on cholera intoxication

CT may promote the cytosolic delivery of CTA1 by inducing the UPR, exploiting UPR effects (such as increased ERAD activity or increased transport), leading to enhanced intoxication measured by increased levels of cytosolic CTA1 and increased concentrations of cAMP.

CHAPTER TWO: MATERIALS AND METHODS

Cell Culture

To passage cells, they were seeded into 10 cm dishes and allowed to grow for 3-4 days at 37°C until 80% confluency was reached. Cells were washed once in 1X PBS and 2 ml of trypsin-EDTA was added to incubate for 5 minutes at 37°C. Then 8 ml of the appropriate media containing 10% fetal bovine serum (FBS) (Invitrogen Carisbad, CA) and 1% antibiotic-antimycotic (Invitrogen) was added to the dish to resuspend cells by tituration. HeLa cells require using Dulbecco's Modified Eagle Medium (DMEM) (Invitrogen). CHO cells use Ham's F12 media (Invitrogen). CHO- beta-2 adrenergic receptor (β_2AR) cells were passaged in media containing a 1:1 ratio of DMEM and F12 as well as 1 mM of sodium selenite. 9 ml of the appropriate media was added to an empty 10 cm dish. 1 ml of the cell resuspension was added to this plate and gently rocked to create an even distribution and bring the final volume to 10 ml.

Cells were seeded onto a 6 well tissue culture plate in a dilution of 4 ml of cell resuspension to 1 ml of media. Cells seeded onto a 24 well tissue culture plate had a dilution of 1 ml of cell resuspension to 5 ml of media. For experiments using 6 well plates, 1 ml of the cell resuspension was added to each well; experiments using 24 well plates had 0.5 ml of the cell resuspension added to each well.

HeLa cells undergoing intoxication required the addition of the GM1 host cell receptor as they lack GM1 surface expression. Cells were washed in serum-free media and incubated with 100 ng/ml GM1 (Sigma-Aldrich St. Lous, MO) in serum-free media for 1 hour at 37°C in order to incorporate the receptor into the membrane. Cells were then washed with serum-free media

and then incubated with the wild-type or mutant toxin in serum-free media for the specified time point.

For experiments requiring activation of Gsα independently of toxin, CHO-β_2AR cells were used. Gsα was activated independently of toxin by stimulating β_2AR expressed on CHO-β_2AR cells. β_2AR was stimulated by chemical treatment with isoproterenol (Sigma-Alderich) at 1 μM in serum-free media for the specified time point. AC was activated independently of toxin by adding forskolin (Sigma-Alderich) at a concentration of 100 μM in serum-free media.

Mutant and wild-type toxins

In order to investigate potential links between UPR activation and the function of CT, we used various CT inactive mutants that are still intact. CTY149S has a single residue mutation, leading to toxin inactivity in mammalian cells (K. Teter, unpublished observations). CTY149S loses the ability to interact with ARF6. To confirm results from experiments using CTY149S were not due to the loss of interaction with ARF6, E110D/E112D mutants were also used. E110D/E112D can still interact with ARF6 but is inactive due to the two active site substitutions (34-36). Results from experiments using mutants were compared to cells treated with wild-type toxin (Sigma-Alderich). Cells exposed to toxin for dual luciferase reporter assay experiments and cAMP assay experiments were treated with CT at 100 ng/ml. Cells exposed to toxin for translocation experiments were treated with CT at 1 μg/ml to account for the low amount of toxin that reaches the ER (37) and to saturate surface binding sites.

Dual Luciferase Reporter Assay

CHO or CHO-β_2AR cells were seeded in 6 well plates in triplicate and incubated overnight at 37°C to 80% confluency. Cells were then washed with serum-free media and transfected with p5xUPRE-GL3 (luciferase reporter construct encoding firefly luciferase controlled by the ATF6/XBP1 binding motif called the unfolded protein response element or UPRE) and pRLSV40P (a constitutive construct encoding *Renilla* luciferase to serve as an internal control for transfection efficiency). An overview of the reporter assay is provided in Figure 3. The transfection solutions were prepared by adding 0.5 µg ATF6 reporter construct and 0.1 µg *Renilla* constitutive construct per 100 µl serum-free media to solution A and 5 µl lipofectamine (Invitrogen Carlsbad, CA) per 100 µl serum-free media to solution B. Solutions A and B were incubated separately for 5 minutes and were then co-incubated at room temperature for 30 minutes. Cells were washed with serum-free media and 200 µl of the transfection mixture was added to each well containing 1 ml fresh serum-free media. After 3 hours of incubation at 37°C, the transfection mixture was removed and cells were incubated overnight at 37°C in antibiotic-free media containing 10% serum. Cells were washed and subjected to the specified experimental conditions in serum-free media.

At the end of the experiment, cells were washed with 1X PBS (phosphate buffered saline) and then luminescence was determined using the Dual-Luciferase Reporter kit (Promega Madison, WI). Cells were incubated with 1X Passive Lysis Buffer (Promega) for 15 minutes with rocking at room temperature to lyse cells. Lysates were transferred to a clear-bottom 96 well black-walled plate (Fisher Scientific Ocala, FL). Luciferase Assay Reagent II (Promega) was added to each well and the firefly luciferase luminescence signal was measured for each

sample using the BioTek Synergy 2 plate reader (Winooski, VT) indicating UPRE induction. The detection setting and emission was set at luminescence and hole, respectively. Stop & Glo (Promega) was then added to each well, which stops the firefly luciferase reaction and simultaneously begins the *Renilla* luciferase reaction to give a signal that was then measured. The *Renilla* construct gives a constitutively active luminescence signal and works as an internal control to account for transfection efficiencies and overall protein translation. The ratio of each sample's *Renilla* luminescence signal to that of the uninduced control was used to normalize the UPRE construct luminescence signal.

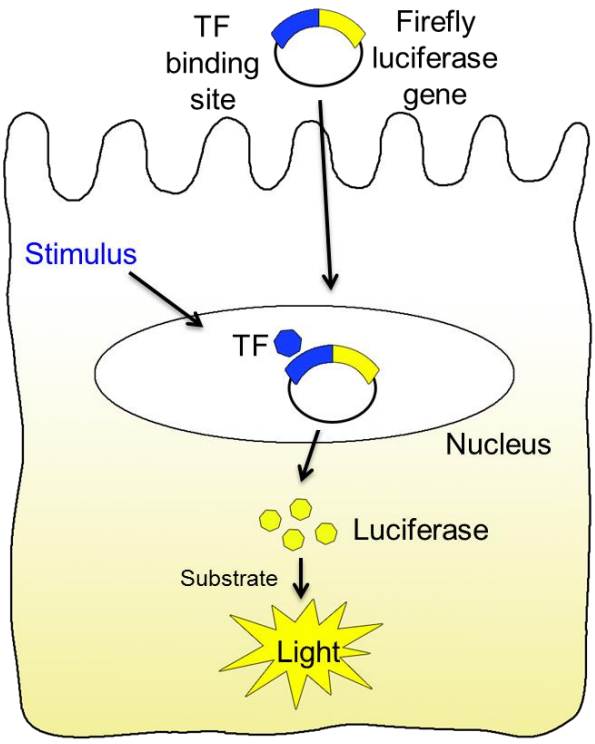

Figure 3: Determining UPR activity by the luciferase reporter assay

Cells are transfected with a construct encoding firefly luciferase and a UPR transcription factor (TF) binding site known as UPRE. Cells are placed under conditions of ER stress, which promotes the activation of UPR TFs. This results in TF binding to the UPRE and the translation of luciferase, which facilitates a measurable luminescent reaction.

cAMP Competition Immunoassay

To measure the effect of intoxication, cellular cAMP was measured by using competition immunoassays. Experimental samples were introduced to a defined amount of anti-cAMP antibodies followed by labeled cAMP. If cellular cAMP concentrations are low, the antibodies bind the more abundant labeled cAMP. Either a radioisotope or a peroxidase is used to label cAMP, depending on the particular kit used. This produces a radioactive or colorimetric signal. When cellular cAMP concentrations increase, it competes with labeled cAMP for binding to the antibodies, which leads to a decrease in labeled cAMP binding and a decrease in the signal observed.

HeLa or CHO-β_2AR cells were seeded in 24 well plates in triplicate and incubated overnight at 37°C to 80% confluency. Cells were washed and subjected to specified experimental conditions in serum-free media at 37°C. Wells were washed with 1X PBS and treated with 250 µl of ice cold HCl:EtOH (1:100) for 10 minutes at 4°C. The samples were transferred to a new 24 well plate and allowed to air dry overnight. Determination of cellular cAMP concentrations was performed with the either the (Perkin Elmer Waltham, MA) cAMP [125I] radioimmunoassay kit or the (GE Healthcare Piscataway, NJ) cAMP Biotrak Enzymeimmunoassay (EIA) kit according to the manufacturer's instructions. The signal obtained from unintoxicated cells was subtracted from the signal of all other conditions. The cAMP signal obtained from unintoxicated cells treated with tunicamycin was also subtracted from the signal obtained from tunicamycin treated intoxicated cells.

Translocation and Digitonin Permeabilization Assay

A digitonin permeabilization assay was performed in order to separate cytosolic fractions (containing cytosolic CTA1) and organelle fractions (containing holotoxin or CTA1 within the ER and other endomembrane compartments) (38). HeLa, CHO, or CHO-β_2AR cells were seeded in 6 well plates in triplicate and incubated overnight at 37°C to 80% confluency. Cells were washed and then underwent a pulse chase experiment in which cells incubated with the wild-type or mutant toxin in serum-free media for 30 min at 4°C. At this temperature intracellular transport is halted, which enables toxin to pulse-label the cells (i.e., binding to the surface of cells without being internalized). Cells were washed with serum-free media to remove unbound toxin and incubated at 37°C to synchronize toxin internalization. Cells were chased in serum-free medium containing no additional treatments or brefeldin A (BfA) at 5 μg/ml for the specified time points. BfA is used as a negative control because it blocks CT delivery to the ER (37). Cells were then washed with 1X PBS and lifted off the plate with 0.5 mM EDTA in 1X PBS (400 μl per well). Three wells used for the same condition were consolidated into one microcentrifuge tube. Samples were centrifuged at 5000 x g for 5 min, and the supernatant was discarded. The pelleted cells were resuspended and treated with 100 μl of chilled 0.04% digitonin (Sigma-Aldrich) in HCN buffer (50 mM Hepes pH 7.5, 150 mM NaCl, 2 mM $CaCl_2$, and 10 mM *N*-ethylmaleimide) to selectively permeabilize the plasma membrane. Samples were incubated on ice for 10 minutes and then centrifuged at 16,000 x g for 10 minutes in order to separate cytosolic (supernatant) fractions from organelle (pellet) fractions. The supernatant fraction was collected into new microcentrifuge tubes.

For samples undergoing Western blot analysis, 120 µl of 1X Sample Buffer was added to the pellet fraction and 20 µl of 4X Sample Buffer was added to the supernatant fraction. For samples undergoing surface plasmon resonance (SPR) analysis, 900 µl of PBS-T (140 mM NaCl, 2.7 mM KCl, 0.05% Tween 20, 10 mM PO_4^{3-}, Medicago Uppsala Sweden) was added to the supernatant fractions to bring the final volume to 1 ml.

Immunoblot of Pellet and Supernatant Fractions

In order to verify that proteins within the pellet (i.e., organelle) fractions obtained from the translocation assay did not contaminate the supernatant fractions, a Western blot was performed against protein markers that reside in either the cytosol or ER. Experimental samples (20 µl) were loaded onto a 15% SDS-PAGE gel. Gels were run at 200 volts for 60 minutes with the (Bio-Rad Hercules, CA) HC power supply. Gels were then incubated in 1X transfer buffer at room temperature for 5 minutes. A PVDF membrane was activated in methanol for 2 minutes, then rinsed in water and incubated in transfer buffer for 10 minutes. One piece of filter paper (pre-soaked in 1X transfer buffer) was placed on the platinum-coated anode of the transfer apparatus (Bio-Rad) followed by the PVDF membrane, the SDS-PAGE gel, and another piece of pre-soaked filter paper to complete the transfer sandwich. The sandwich was rolled over to eliminate air bubbles. The cathode of the transfer apparatus was secured, and the transfer was allowed to proceed at 10 volts for 20 minutes followed by 15 volts for 40 minutes using the HC power supply (Bio-Rad).

Membranes were blocked for 20 minutes in 5% milk in 1X TBST (15 mM Tris pH 7.5, 150 mM NaCl, 0.1% Tween 20, H_2O) at room temperature. Membranes were then rinsed with

1% milk in 1X TBST and incubated with primary antibody (rabbit anti-PDI 1:5,000; rabbit anti-HSP90 1:10,000; Stressgen Farmingdale, NY) in 1% milk in 1X TBST overnight on a rocker at 4°C. Membranes were washed three times in 1% milk in 1X TBST for 10 minutes each time on a rocker at room temperature. Membranes were then incubated with secondary antibody (goat anti-rabbit horseradish peroxidase-conjugated 1:10,000; Jackson Immuno West Grove, PA) for 1 hour on a rocker at room temperature. The membrane was washed three times in 1% milk in 1X TBST for 10 minutes on a rocker at room temperature. ECL Plus Western Blotting Detection Reagents (GE Healthcare) was used to detect the presence of proteins according to the manufacturer's instructions.

SPR Slide Preparation and Sample Analysis

Cytosolic samples obtained from translocation assays were analyzed by SPR, which allows for the detection of cytosolic CTA1. Antibodies against CTA1 are immobilized on a sensor slide. When CTA1 in the sample binds to the antibody, there is a change in the reflection of light. This change can be measured and converted into a trace on a sensorgram, plotting time as a function of refractive index unit (RIU). An increase in RIU represents an interaction between CTA1 and anti-CTA1 antibody and thus indicates the presence of CTA1 within a given sample. An overview of the SPR detection system is provided in Figure 4.

To prepare the sensor slide, a gold-plated glass slide (Reichert Depew, NJ) was mounted onto the prism surface of the SR7000 SPR Refractometer (Reichert). The slide was activated with an EDC-NHS (Thermo Scientific Waltham, MA) solution by injecting the solution into the inject port and allowing the solution to perfuse over the slide through the flow channel for 5

minutes. The slide was subsequently washed by perfusing PBS-T for 5 minutes. Monoclonal anti-CTA1 antibody 35C2 (39) at a ratio of 1:20,000 in 20 nM sodium acetate (pH 5.5) was then perfused over the slide for 5 minutes. The slide was washed with PBS-T for 5 minutes to remove unbound antibodies. To block unbound reactive tethers on the slide, 1 M ethanolamine (pH 8.5) was perfused for 2 minutes. The slide was washed in PBST for 5 minutes to establish a baseline RIU signal.

Experimental samples were perfused over the slide for 5 minutes and then washed for 5 minutes in PBST to remove the analyte. Perfusions had a flow rate of 41 µl/min and injections were 1 ml each. The sensorgram of all samples were generated using LabVIEW (Reichert), Scrubber 2 (BioLogic Campbell, Australia), and Igor (WaveMetrics, Lake Oswego, Oregon) software.

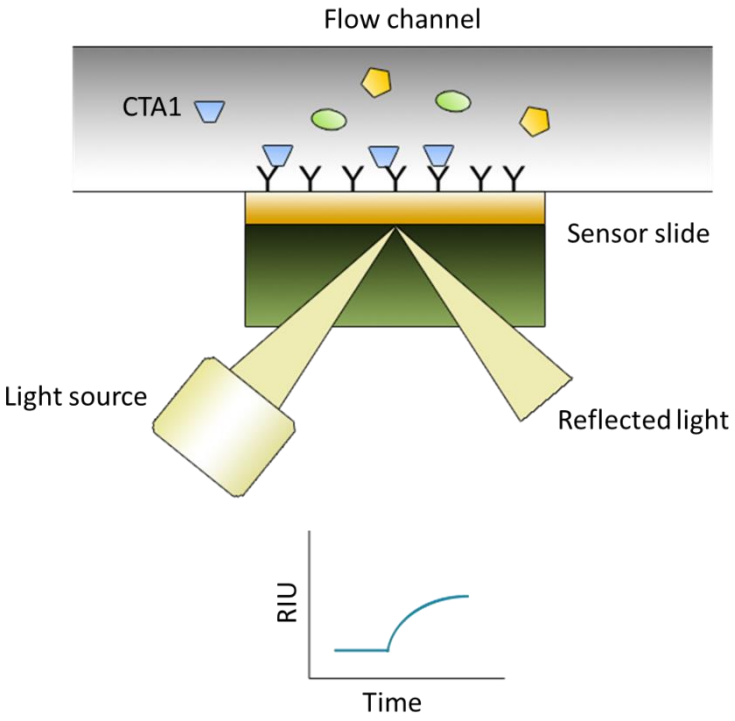

Figure 4: SPR as a detection method to analyze presence of CTA1 in cytosol

Cytosolic samples are obtained and injected into the flow channel. When CTA1 interacts with fixed anti-CTA1 antibody, the incident angle of light changes and can be measured. This change in reflected light is converted into a trace onto a sensorgram which plots the RIU over time. An increase in RIU indicates interaction between the antibody and the CTA1 analyte.

CHAPTER THREE: RESULTS

UPR induction by CT correlates with enhanced intoxication

The activation of the UPR by Shiga toxin and ricin appears to be dependent on toxin function. Ricin inhibited UPR activation which led to enhanced cytotoxicity, however inactive mutants of ricin were not able to inhibit UPR activation (29). Shiga toxin stimulates an UPR, but this regulation also enhances intoxication. Again, an active Shiga toxin was necessary to induce the UPR (28). Preliminary data of luciferase reporter assays has shown that wild-type CT was able to induce an UPR after 4 hr of intoxication (A. Grabon and K. Teter, unpublished manuscript). However CTY149S, the inactive mutant toxin in mammalian cells, was not able to induce the UPR. In this section we tested the hypothesis that UPR activation by an active CT enhances intoxication.

We measured the level of intoxication by monitoring the amount of cytosolic CTA1 present in HeLa cells. This was determined by a process involving digitonin permeabilization coupled with SPR analysis as described in the Methods section. Using digitonin allows for the selective permeabilization of the plasma membrane while leaving the membranes of organelles intact. The fidelity of our samples needed to be verified in order to ensure the specific collection of cytosolic CTA1 in the supernatant fraction (and not CTA1 within membrane bound compartments). We performed a digitonin permeabilization assay to separate organelle (pellet, P) and cytosol (supernatant, S) fractions which were then tested for the presence of protein markers that are known to reside in organelles or in the cytosol. Protein disulfide isomerase (PDI), a soluble ER resident protein, remained in the pellet and heat shock protein 90 (Hsp90), a cytosolic protein, was maintained in supernatant (Figure 5). A small pool of Hsp90 was associated with

the membrane pellet which accounts for the faint band in the P fraction. This minor pool of membrane-associated Hsp90 was also observed by others (38). Thus, the Western blot confirmed sample fidelity by revealing that the membrane bound organelles remain intact, which allows for subsequent sample analysis through SPR.

Cytosolic fractions were analyzed for the presence of CTA1 in HeLa cells exposed to wild-type CT and one of two inactive CT mutants: CT Y149S (Figure 6A) or CT E110D/E112D (Figure 6B). The SPR sensorgrams reveal that cytosolic CTA1 levels for cells intoxicated with mutant CT are similar to that of cells intoxicated with wild-type CT at 1 and 4 hr of chase (Figures 6A-B). However, the marked increase in cytosolic CTA1 observed for wild-type CT at 5 hr of chase was not seen for either mutant toxin. No signal was observed for unintoxicated or BfA-treated cells, two negative controls. Unintoxicated cells serve as a reference because since no toxin was added to the cells, there is no CTA1 within the cytosolic sample that reacts with the anti-CTA1 antibody fixed onto the SPR sensor slide. BfA-treated cells are intoxicated with CT, but BfA treatment blocks entry of CT to the ER and thus should produce minimal to no signal as CT would not enter the cytosol. The significant increase in cytosolic CTA1 after 4 hr of exposure to wild-type CT coincides with UPR activation with wild-type CT after 4 hr of intoxication with wild-type CT but not with CT149S (A. Grabon and K. Teter, unpublished observations). This data suggests that wild-type CT activates the UPR to enhance cytosolic delivery of toxin and therefore enhance toxicity.

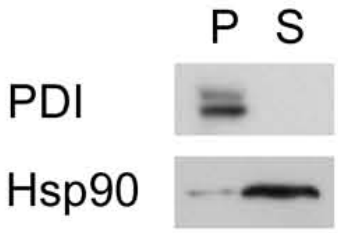

Figure 5: Organelle and cytosol fractions are tested for the presence of protein markers

HeLa cells were grown to 80% confluence in 6 well plates and then gently lifted from the plates using 5 mM EDTA in 1X PBS. Collected cells were centrifuged at 5000 x g for 5 min and then selectively permeabilized with 0.04% digitonin in HCN buffer. Another centrifugation at 16,000 x g for 10 min was used to separate pellet (P, organelle) and supernatant (S, cytosol) fractions. Pellet and supernatant fractions underwent Western blot analysis to determine the distribution of PDI and Hsp90 in each fraction. Anti-PDI antibody, 1:5000. Anti-Hsp90 antibody, 1:10,000.

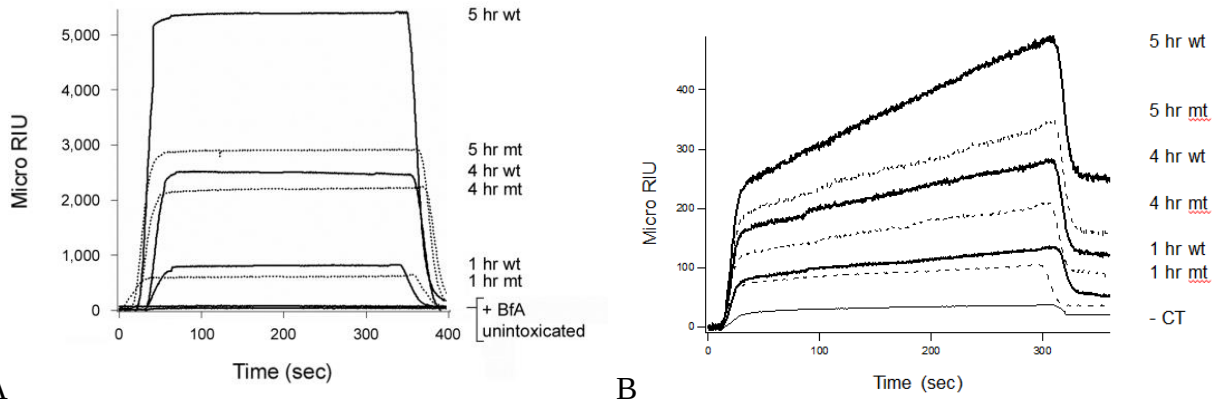

Figure 6: SPR sensorgram of HeLa cells after wild-type or mutant toxin exposure

After 4 hr of intoxication, there is a marked increase in cytosolic CTA1 for cells intoxicated with wild-type. HeLa cells were pulse-labeled with wild-type (A-B), mutant CTY149S (A), or mutant E110D/E112D (B) at 4°C for 30 min at 1 μg/ml. After unbound toxin was removed, cytosolic fractions were chased after 1, 4, and 5 hr. The BfA treated sample was chased after 1 hr. The sensorgram shown in A is a representative figure from two independent experiments. The data depicted in B is representative from three independent experiments. BfA treated cells are used as a control as BfA blocks CT delivery to the ER. Unintoxicated cells, -CT. Wild-type, wt. Mutant, mt.

Chemical UPR activation enhances intoxication

If CT activation of the UPR leads to increased toxin in the cytosol, then chemical activation of the UPR should yield similar results. To determine if CT-induced UPR activity has the same effect on cytosolic CTA1 as does chemically induced UPR activity, HeLa cells underwent UPR pre-activation with tunicamycin and then cytosolic CTA1 was examined. Tunicamycin is another chemical used to activate the UPR by inhibiting *N*-glycosylation, thus leading to the accumulation of misfolded proteins and ER stress. In non-UPR-activated cells (i.e. without tunicamycin treatment), CTA1 was detected in the cytosolic fraction at 30 min but not at 15 min (Figure 7A). There is a gradual increase in cytosolic CTA1 at each subsequent time point. UPR-activated (i.e. tunicamycin treated) cells exported CTA1 into the cytosol sooner and at higher amounts compared to that of non-treated cells (Figure 7B). In UPR-activated cells, CTA1 is even detected after only 15 min, with an increase in cytosolic CTA1 at each subsequent time point as observed for non-UPR activated cells. Unintoxicated cells or cells treated with BfA show no signal.

In order to quantify cytosolic CTA1 in SPR sensorgrams, we used Scrubber 2 software to extrapolate association rate constants (k_a) from SPR data of samples and standards of known CTA concentration. A standard curve was generated, plotting k_a as a function of protein concentration. The slope of the curve was then used to determine CTA1 concentration for experimental samples (Figure 7C). The resulting qualitative data confirmed that greater levels of CTA1 arrive in the cytosol sooner in tunicamycin treated cells than in untreated cells. Thus, these data suggest that UPR activation induced by chemical and by toxin enhances toxicity within cells.

Since UPR induction enhanced cytosolic CTA1 levels, we tested the hypothesis that tunicamycin would also increase the levels of cAMP during intoxication. HeLa cells were pre-treated with tunicamycin for 90 min and then exposed to CT continuously for 2 hr (Figure 8). Tunicamycin pre-treatment increased cAMP concentrations during intoxication by 2.4 fold when compared to intoxicated HeLa cells that were not pre-treated with tunicamycin. Thus, UPR activation sensitizes HeLa cells to intoxication by increasing cytosolic CTA1 and, in turn, increasing cAMP concentrations.

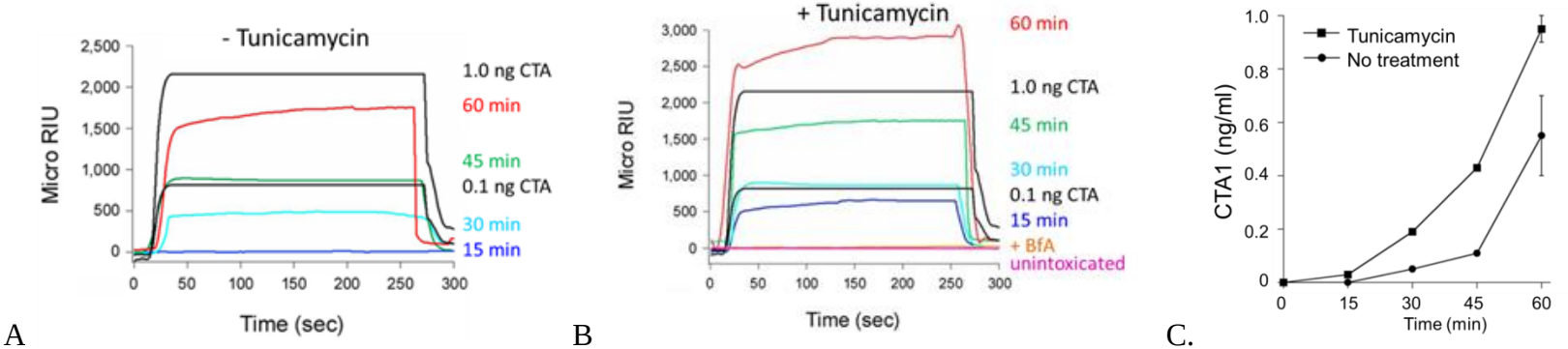

Figure 7: The effect of chemical UPR induction on the levels of cytosolic CTA1

Cytosolic CTA1 in tunicamycin absent (non-UPR activated, A) or tunicamycin treated (UPR activated, B) cells. HeLa cells were treated in the absence or presence of 10 µg/ml tunicamycin for 90 min at 37°C. Cells were pulse-labeled with 1 µg/ml wild-type CT at4°C for 30 min. Cytosolic CTA1 was then chased at 37°C after the specified time point and analyzed by SPR. CTA traces in black indicate 1 and 0.1 ng CTA1 standards. The SPR sensorgrams are representative of two independent experiments. (C) Quantification of cytosolic CTA1 from cells treated with or without tunicamycin using Scrubber 2 software.

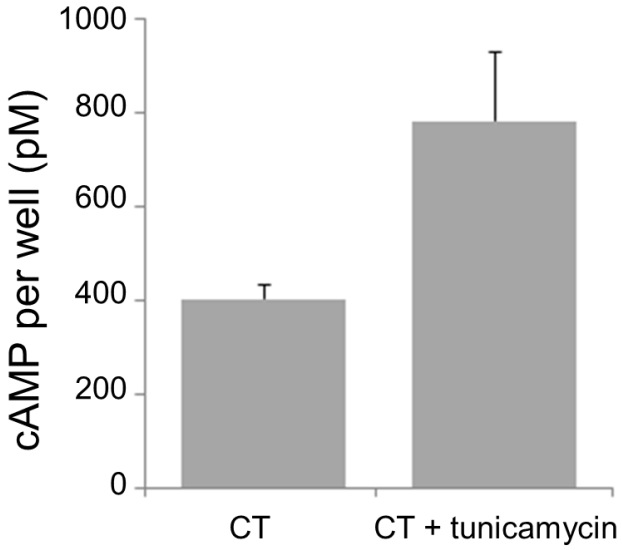

Figure 8: cAMP concentrations after two hours of intoxication in UPR activated cells

HeLa cells were treated with or without 10 µg/ml tunicamycin for 90 min at 37°C and subsequently incubated with or without CT (100 ng/ml) continuously for 2 hours at 37°C. Cellular cAMP concentrations were then determined. The experiment was performed once with triplicate samples.

CT-induced UPR activation occurs independently of AC

CT is able to induce an UPR, and this induction is dependent on CT activity (A. Grabon and K. Teter, unpublished observations). Active CT locks Gsα in an active state, which consequently leads to continual stimulation of AC and the production of high levels of cAMP. We investigated whether UPR activation during intoxication is dependent on cAMP or on Gsα. To determine the role of AC or Gsα on UPR activity, UPR activity was measured after AC and Gsα were stimulated by chemical treatment. To stimulate AC and Gsα independently of CT, we utilized CHO-β_2AR cells and treated them with forskolin to activate AC and isoproterenol to activate Gsα. Isoproterenol is a chemical that activates the G-coupled protein receptor, β_2AR, which is stably expressed on CHO-β_2AR cells.

Control experiments verified that cAMP pathways were active in CHO-β_2AR cells (Figure 9). Treatment with thapsigargin alone for either 90 min or 4 hr had minimal effect on cAMP levels. In contrast, CHO-β_2AR cells challenged with CT, forskolin, or isoproterenol exhibited considerably increased cAMP concentrations (Figure 9). This indicated that the CT, AC, and Gsα pathways were functional in CHO-β_2AR cells. While CHO-β_2AR cells produced increased cAMP concentrations in response to isoproterenol, CHO cells without expressed β_2AR did not have a cAMP increase in response to isoproterenol (data not shown).

CHO-β_2AR cells were analyzed for UPR activity by a luciferase assay after challenging cells with forskolin, isoproterenol, thapsigargin, and wild-type CT (Figure 10). The reporter assay demonstrated that 4 hr of wild-type CT exposure induces UPR activity, as did the positive control thapsigargin. Forskolin treatment did not result in UPR activation, whereas isoproterenol treatment induced UPR activity. In other words, Gsα activation induced an UPR while AC

activation did not. Since both forskolin and isoproterenol generated elevated cAMP levels but only isoproterenol activated the UPR, elevated cAMP is not responsible for UPR activation.

Since UPR induction enhances the cytosolic delivery of CTA1, we tested the hypothesis that Gsα activation also stimulates the delivery of CTA1 to the host cytosol. A control experiment was performed in CHO-β_2AR cells in order to determine at what point cytosolic CTA1 is detected in the cytosol of intoxicated cells (Figure 11A). Cytosolic CTA1 was not observed at 30 min of chase, but was observed at 45 min of chase. We predicted that UPR activation would enhance toxin delivery in CHO-β_2AR cells and allow detection of CTA1 after only 30 min of chase. CHO-β_2AR cells were pre-activated with thapsigargin, forskolin, or isoproterenol for 90 min or 4 hr. After pulse-labeling with wild-type CT, cytosolic fractions were collected from untreated and drug-treated cells after 30 min of toxin exposure. Samples were analyzed by SPR to determine if pre-activation of the UPR produced a cytosolic pool of CTA1 after just 30 min of chase. Cytosolic CTA1 was detected after only 30 min of chase for cells treated with isoproterenol and thapsigargin, but not for forskolin-treated cells or untreated cells (Figure 11B-C). CHO cells not expressing β_2AR did not have an increase in cytosolic CTA1 after isoproterenol treatment (data not shown). These data suggest that Gsα-induced UPR activation enhances the levels of cytosolic CTA1 in a process that is independent of the cAMP signaling pathway.

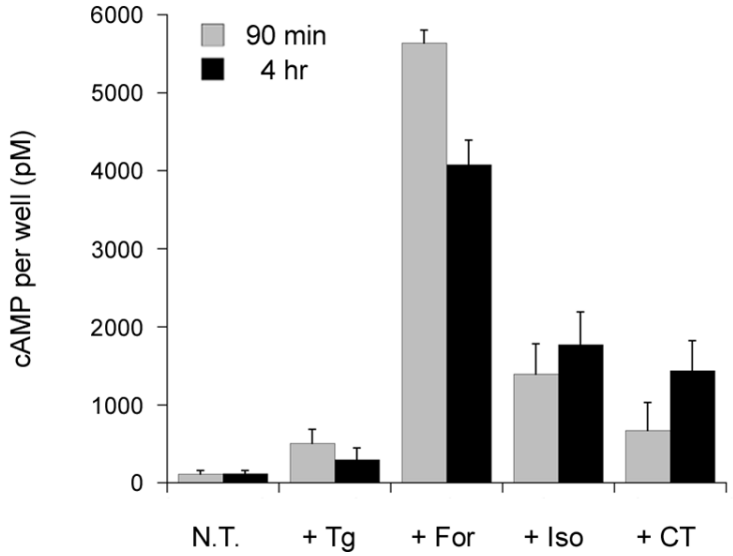

Figure 9: cAMP assay to verify cAMP production in CHO-β_2AR cells

CHO-β_2AR cells were treated with 200 nM thapsigargin (Tg), 100 µM forskolin (For), 1 µM isoproterenol (Iso), or 100 ng/ml wild-type CT for 4 hr. Cellular cAMP levels were then determined. The data represents the average of two independent experiments.

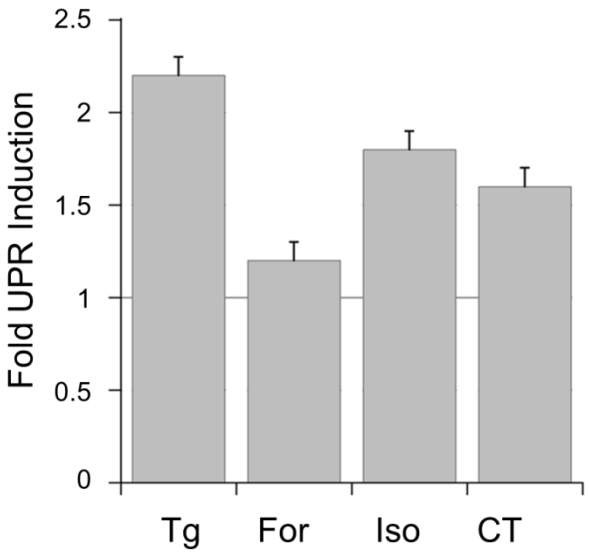

Figure 10: The ability of AC and Gsα to induce an UPR

CHO-β_2AR cells were transfected with the p5xUPRE-GL3 luciferase reporter construct and then challenged for 4 hr with 100 ng/ml wild-type CT, 200 nM thapsigargin, 100 µM forskolin, or 1 µM isoproterenol. Luciferase reaction luminescence was then measured. The data represents the average of four independent experiments.

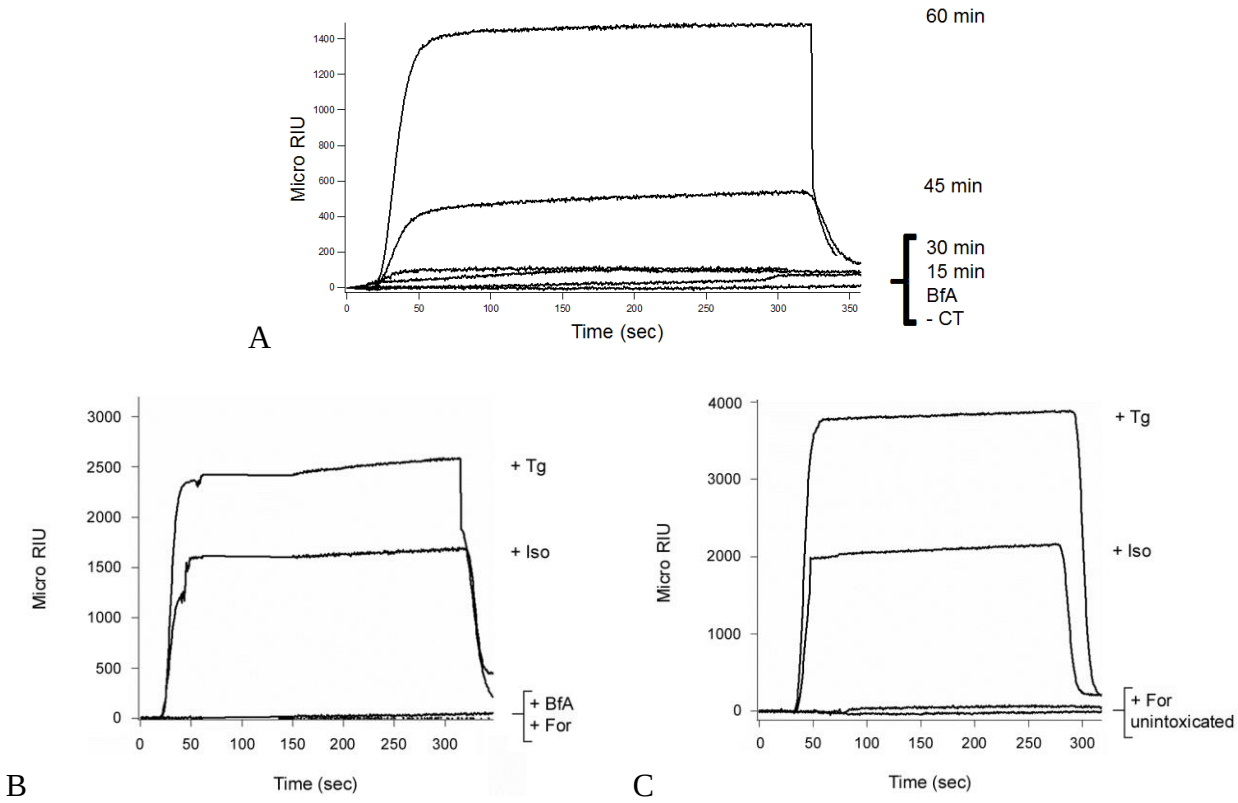

Figure 11: The effect of Gsα and AC activation on cytosolic CTA1 delivery to the cytosol

(A) CHO-β_2AR cells were pulse-labeled with 1 μg/ml of wild-type CT at 4°C for 30 min. Cytosolic fractions were then collected after the specified time point at 37°C and analyzed by SPR. (B-C) CHO-β_2AR cells pre-treated with 200 nM thapsigargin, 100 μM forskolin, or 1 μM isoproterenol for 90 min (B) or 4 hr (C) before pulse-labeling with wild-type CT. Cytosolic fractions were collected after 30 min at 37°C and analyzed by SPR. The sensorgrams from B and C are representative figures from two independent experiments.

CHAPTER FOUR: DISCUSSION

The activity of AB toxins is linked to UPR induction

The UPR has a role in the pathogenesis caused by several toxins, but its involvement has not been extensively studied for CT. In the present study, CT-induced UPR activation occurred within CHO-β_2AR cells (Figure 10). UPR activation in turn enhanced intoxication by increasing cytosolic CTA1 (Figure 7) and cellular cAMP concentrations (Figure 8). Preliminary data found in CHO cells (A. Grabon and K. Teter, unpublished observations) also show UPR induction by wild-type CT and demonstrate the inability of the inactive mutant to induce an UPR, which suggests CTA1 activity leads to an UPR.

CTA1 traffics to the ER where it is recognized as a misfolded protein for translocation into the cytosol. The UPR is induced due to the presence of misfolded proteins within the ER. Consequently, it is tempting to draw a link between the presence of CTA1 within the ER and UPR, but this is unlikely because of the small pool of internalized CT that actually makes it to the ER (37). UPR induction likely depends on toxin function. To support this, the mutant toxins that were unable to induce an UPR were detected in the cytosol (Figure 6), so the mere presence of toxin within the ER is not sufficient to induce an UPR.

Active Shiga toxin and ricin also modulate the UPR, and this regulation was linked to toxin activity (28, 29). Shiga toxin may induce the UPR through inactivation of ribosomes by its enzymatic A1 subunit (STxA1). The resulting protein synthesis inhibition possibly contributes to a deficit of chaperones within the ER, contributing to ER stress. The mode of action for CT does not involve ribosome inactivation, but rather the modification of Gsα, leading to AC hyperactivation and increased cAMP concentrations.

We investigated the link between CT activity and UPR induction, specifically examining the role of the cAMP pathway. CT induced an UPR, but treatment with the AC agonist forskolin did not activate the UPR (Figure 10). Additionally, forskolin treatment did not increase the pool of cytosolic CTA1. In contrast, treatment with the global UPR inducers tunicamycin (Figure 7) and thapsigargin (Figure 11) enhanced the rate of CTA1 delivery to the cytosol. Thus, UPR induction in response to CT and the resulting sensitization of cells to toxin likely occurs via an AC-independent mechanism. Other studies have also shown cAMP-independent signaling events driven by CT (40, 41), but these events were not directly related to the CT intoxication process.

To investigate if UPR induction was occurring upstream of AC, Gsα activation by isoproterenol was used. In contrast to AC activation, Gsα activation induced UPR activity (Figure 10) as well as increased cytosolic CTA1 (Figure 11). UPR activity through Gsα would represent an unexpected mechanism for CT-induced UPR activity instead of the typical ER stress pathway. UPR activation by pore forming toxins was also found to occur independently of ER stress through the p38 mitogen-activated protein kinase (MAPK) signaling pathway (42). G-protein signaling can activate p38 MAPK (43), so we investigated if p38 had a role in CT-induced UPR activity; however we found that a p38 inhibitor, SB203580, did not block cAMP production after 5 hr of toxin exposure (data not shown).

UPR induction results in enhanced intoxication

Toxin induced-UPR by Shiga toxin and ricin sensitizes mammalian and yeast cells to cytotoxicity (28, 29). We similarly found that UPR induction enhances intoxication. UPR induction by global UPR inducers enhances delivery of CTA1 to cytosol (Figures 7, 11).

Chemically induced UPR also increased cAMP concentrations during intoxication in HeLa cells (Figure 8) and CHO cells (A. Grabon and K. Teter, unpublished observations). Other investigators have also demonstrated enhanced cholera intoxication in response to thapsigargin (32) and tunicamycin (44). Thus, the UPR sensitizes cells to the effects of intoxication.

Analysis of cytosolic CTA1 by SPR has consistently shown a marked increase in CTA1 after 4 hr of chase (18). UPR activation by wild-type and not mutant CT also occurs at 4 hr of toxin exposure (A. Grabon and K. Teter, unpublished observations). We tested whether intoxication by the mutant CT, which could not induce the UPR, would also result in marked levels of cytosolic CTA1 after 4 hr. While CTA1 from mutant CT was detected in the cytosol at similar levels as wild-type toxin at 1 and 4 hr, the marked increase observed for wild-type CTA1 at 5 hr was not observed for mutant. Thus, the marked increase typical for cells intoxicated with wild-type CT at 5 hr may be due to the time it takes for the UPR to be induced.

The ERAD pathway and the UPR are linked, so it is possible that enhanced intoxication occurs during an UPR due to increased ERAD activity. This seems unlikely due to our SPR data demonstrating the time in which we begin to see CTA1 in the cytosol (Figure 7). No CTA1 was detected after 15 min of chase in non-UPR activated cells. After 15 min of chase, the concentration of cytosolic CTA1 in UPR-activated cells is approximately equal to that observed for the 30 min chase of non-UPR activated cells; the concentration after 30 min of chase is similar to that of the 45 min, etc. If the UPR was affecting ERAD during intoxication, the lag time for toxin to reach the cytosol would not be affected. Instead, UPR induction may enhance trafficking, which is supported by another study showing increased transport to the ER after thapsigargin treatment (32).

CHAPTER FIVE: CONCLUSION

After 4 hr of cholera intoxication, the UPR is activated which is thought to cause the jump in cytosolic CTA1 levels after 4 hr. To support this, UPR pre-activation by chemical means results in enhanced intoxication. UPR activation by CT is AC-independent, but may be dependent on Gsα as Gsα activation induced an UPR independently of toxin.

These data suggest a novel role for the UPR, which is enhanced cholera intoxication via an AC-independent mechanism and further demonstrates how pathogens exploit multiple host processes in order to cause disease. Future studies will investigate the involvement of the three UPR pathways during intoxication as well the involvement of Gsα during toxin-induced UPR.

LIST OF REFERENCES

1. Sack DA, Sack RB, Nair GB, Siddique AK. Cholera. Lancet. 2004 Jan;363(9404):223-33. PubMed PMID: WOS:000188243900023.

2. Gaffga NH, Tauxe RV, Mintz ED. Cholera: A new homeland in Africa? American Journal of Tropical Medicine and Hygiene. 2007 Oct;77(4):705-13. PubMed PMID: WOS:000250244800022.

3. Guerrant RL, Carneiro BA, Dillingham RA. Cholera, diarrhea, and oral rehydration therapy: Triumph and indictment. Clinical Infectious Diseases. 2003 Aug 1;37(3):398-405. PubMed PMID: WOS:000184407900012.

4. Middlebrook JL, Dorland RB. Bacterial Toxins - Cellular Mechanisms of Action. Microbiological Reviews. 1984 1984;48(3):199-221. PubMed PMID: WOS:A1984TJ71900002.

5. Sixma TK, Pronk SE, Kalk KH, Wartna ES, Vanzanten BAM, Witholt B, et al. Crystal structure of a cholera toxin-related heat-labile enterotoxin from *E. coli*. Nature. 1991 May 30;351(6325):371-7. PubMed PMID: WOS:A1991FN85600047.

6. Rappuoli R, Pizza M, Douce G, Dougan G. Structure and mucosal adjuvanticity of cholera and Escherichia coli heat-labile enterotoxins. Immunology Today. 1999 Nov;20(11):493-500. PubMed PMID: WOS:000083404500006.

7. Moss J, Fishman PH, Manganiello VC, Vaughan M, Brady RO. Functional incorporation of ganglioside into intact cells: induction of choleragen responsiveness. Proceedings of the National Academy of Sciences of the United States of America. 1976 1976;73(4):1034-7. PubMed PMID: WOS:A1976BP03900015.

8. Jobling MG, Yang Z, Kam WR, Lencer WI, Holmes RK. A single native ganglioside GM1-binding site is sufficient for cholera toxin to bind to cells and complete the intoxication pathway. mBio. 2012 2012 Oct;3(6). PubMed PMID: MEDLINE:23111873.

9. Sandvig K, van Deurs B. Transport of protein toxins into cells: pathways used by ricin, cholera toxin and Shiga toxin. Febs Letters. 2002 Oct 2;529(1):49-53. PubMed PMID: WOS:000178468300010.

10. Chinnapen DJF, Chinnapen H, Saslowsky D, Lencer WI. Rafting with cholera toxin: endocytosis and trafficking from plasma membrane to ER. Fems Microbiology Letters. 2007 Jan;266(2):129-37. PubMed PMID: WOS:000242785200001.

11. Pande AH, Scaglione P, Taylor M, Nemec KN, Tuthill S, Moe D, et al. Conformational instability of the cholera toxin A1 polypeptide. Journal of Molecular Biology. 2007 Dec 7;374(4):1114-28. PubMed PMID: WOS:000251700900023.

12. Jobling MG, Holmes RK. Identification of motifs in cholera toxin A1 polypeptide that ave required for its interaction with human ADP-ribosylation factor 6 in a bacterial two-hybrid system. Proceedings of the National Academy of Sciences of the United States of America. 2000 Dec 19;97(26):14662-7. PubMed PMID: WOS:000165993700120.

13. Teter K, Jobling MG, Sentz D, Holmes RK. The cholera toxin A1(3) subdomain is essential for interaction with ADP-ribosylation factor 6 and full toxic activity but is not required for translocation from the endoplasmic reticulum to the cytosol. Infection and Immunity. 2006 Apr;74(4):2259-67. PubMed PMID: WOS:000236477000029.

14. O'Neal CJ, Jobling MG, Holmes RK, Hol WGJ. Structural basis for the activation of cholera toxin by human ARF6-GTP. Science. 2005 Aug 12;309(5737):1093-6. PubMed PMID: WOS:000231230100051.

15. Cassel D, Pfeuffer T. Mechanism of cholera toxin action: Covalent modification of the guanyl nucleotide-binding protein of the adenylate cyclase system. Proceedings of the National Academy of Sciences of the United States of America. 1978 1978;75(6):2669-73. PubMed PMID: WOS:A1978FF05900030.

16. Gill DM, Meren R. ADP-ribosylation of membrane proteins catalyzed by cholera toxin: basis of the activation of adenylate cyclase. Proceedings of the National Academy of Sciences of the United States of America. 1978 1978;75(7):3050-4. PubMed PMID: WOS:A1978FJ88100011.

17. Lencer WI, Tsai B. The intracellular voyage of cholera toxin: going retro. Trends in Biochemical Sciences. 2003 Dec;28(12):639-45. PubMed PMID: WOS:000187437600004.

18. Massey S, Banerjee T, Pande AH, Taylor M, Tatulian SA, Teter K. Stabilization of the Tertiary Structure of the Cholera Toxin A1 Subunit Inhibits Toxin Dislocation and Cellular Intoxication. Journal of Molecular Biology. 2009 Nov 13;393(5):1083-96. PubMed PMID: WOS:000271596500008.

19. Teter K, Holmes RK. Inhibition of endoplasmic reticulum-associated degradation in CHO cells resistant to cholera toxin, Pseudomonas aeruginosa exotoxin A, and ricin. Infection and Immunity. 2002 Nov;70(11):6172-9. PubMed PMID: WOS:000178675100032.

20. Hazes B, Read RJ. Accumulating evidence suggests that several AB-toxins subvert the endoplasmic reticulum-associated protein degradation pathway to enter target cells. Biochemistry. 1997 Sep 16;36(37):11051-4. PubMed PMID: WOS:A1997XW73300001.

21. Rodighiero C, Tsai B, Rapoport TA, Lencer WI. Role of ubiquitination in retro-translocation of cholera toxin and escape of cytosolic degradation. Embo Reports. 2002 Dec;3(12):1222-7. PubMed PMID: WOS:000180099300022.

22. Yu M, Haslam DB. Shiga toxin is transported from the endoplasmic reticulum following interaction with the luminal chaperone HEDJ/ERdj3. Infection and Immunity. 2005 Apr;73(4):2524-32. PubMed PMID: WOS:000227975000070.

23. Johannes L, Roemer W. Shiga toxins - from cell biology to biomedical applications. Nature Reviews Microbiology. 2010 Feb;8(2):105-16. PubMed PMID: WOS:000273659700010.

24. Parker MW, Feil SC. Pore-forming protein toxins: from structure to function. Progress in Biophysics & Molecular Biology. 2005 May;88(1):91-142. PubMed PMID: WOS:000226499600003.

25. Bernales S, Papa FR, Walter P. Intracellular signaling by the unfolded protein response. Annual Review of Cell and Developmental Biology. 2006;22:487-508.

26. Travers KJ, Patil CK, Wodicka L, Lockhart DJ, Weissman JS, Walter P. Functional and genomic analyses reveal an essential coordination between the unfolded protein response and ER-associated degradation. Cell. 2000 Apr 28;101(3):249-58. PubMed PMID: WOS:000086741900005.

27. Lee A-H, Iwakoshi NN, Glimcher LH. XBP-1 regulates a subset of endoplasmic reticulum resident chaperone genes in the unfolded protein response. Molecular and Cellular Biology. 2003;23(21):7448-59. PubMed PMID: BACD200300336514.

28. Lee S-Y, Lee M-S, Cherla RP, Tesh VL. Shiga toxin 1 induces apoptosis through the endoplasmic reticulum stress response in human monocytic cells. Cellular Microbiology. 2008 Mar;10(3):770-80. PubMed PMID: WOS:000252897000018.

29. Parikh BA, Tortora A, Li X-P, Tumer NE. Ricin inhibits activation of the unfolded protein response by preventing splicing of the HAC1 mRNA. Journal of Biological Chemistry. 2008 Mar 7;283(10):6145-53. PubMed PMID: WOS:000253779500021.

30. Horrix C, Raviv Z, Flescher E, Voss C, Berger MR. Plant ribosome-inactivating proteins type II induce the unfolded protein response in human cancer cells. Cellular And Molecular Life Sciences: CMLS. 2011;68(7):1269-81. PubMed PMID: 20844919.

31. Chao-Ting W, Jetzt AE, Ju-Shun C, Cohick WS. Inhibition of the Unfolded Protein Response by Ricin A-Chain Enhances Its Cytotoxicity in Mammalian Cells. Toxins. 2011;3(5):453-68. PubMed PMID: 60983219.

32. Sandvig K, Garred O, vanDeurs B. Thapsigargin-induced transport of cholera toxin to the endoplasmic reticulum. Proceedings of the National Academy of Sciences of the United States of America. 1996 Oct 29;93(22):12339-43. PubMed PMID: WOS:A1996VP93700053.

33. Coe H, Michalak M. Calcium binding chaperones of the endoplasmic reticulum. General Physiology and Biophysics. 2009;28(Sp. Iss. SI):F96-F103. PubMed PMID: BACD201000113384.

34. Jobling MG, Holmes RK. Biological and biochemical characterization of variant A subunits of cholera toxin constructed by site-directed mutagenesis. Journal of Bacteriology. 2001;183(13):4024-32. PubMed PMID: BACD200100212180.

35. Guimaraes CP, Carette JE, Varadarajan M, Antos J, Popp MW, Spooner E, et al. Identification of host cell factors required for intoxication through use of modified cholera toxin. Journal of Cell Biology. 2011;195(5):751-64. PubMed PMID: BACD201200032822.

36. Teter K, Allyn RL, Jobling MG, Holmes RK. Transfer of the cholera toxin A1 polypeptide from the endoplasmic reticulum to the cytosol is a rapid process facilitated by the endoplasmic reticulum-associated degradation pathway. Infection and Immunity. 2002;70(11):6166-71. PubMed PMID: BACD200300005759.

37. Orlandi PA, Curran PK, Fishman PH. Brefeldin A blocks the response of cultured cells to cholera toxin. Implications for intracellular trafficking in toxin action. The Journal Of Biological Chemistry. 1993;268(16):12010-6. PubMed PMID: 8389369.

38. Taylor M, Banerjee T, VanBennekom N, Teter K. Detection of toxin translocation into the host cytosol by surface plasmon resonance. Journal of visualized experiments : JoVE. 2012 2012 Jan(59):e3686-e. PubMed PMID: MEDLINE:22231143.

39. Holmes RK, Twiddy EM. Characterization of monoclonal antibodies that react with unique and cross-reacting determinants of cholera enterotoxin and its subunits. Infection And Immunity. 1983;42(3):914-23. PubMed PMID: 6196297.

40. Qureshi SA, Alexandropoulos K, Joseph CK, Spangler R, Foster DA. Cholera toxin induces expression of the immediate-early response gene JE via a cyclic AMP-independent

signaling pathway. Molecular And Cellular Biology. 1991;11(1):102-7. PubMed PMID: 1702510.

41. McCloskey MA. Cholera Toxin Potentiates IgE-Coupled Inositol Phospholipid Hydrolysis and Mediator Secretion by RBL-2H3 Cells. Proceedings of the National Academy of Sciences of the United States of America. 1988 (19):7260. PubMed PMID: edsjls.10.2307.32111.

42. Bischof LJ, Kao C-Y, Los FCO, Gonzalez MR, Shen Z, Briggs SP, et al. Activation of the Unfolded Protein Response Is Required for Defenses against Bacterial Pore-Forming Toxin In Vivo. Plos Pathogens. 2008 Oct;4(10). PubMed PMID: WOS:000261481100009.

43. Schulte G, Fredholm BB. Signalling from adenosine receptors to mitogen-activated protein kinases. Cellular Signalling. 2003;15(9):813-27. PubMed PMID: BACD200300267928.

44. Dixit G, Mikoryak C, Hayslett T, Bhat A, Draper RK. Cholera toxin up-regulates endoplasmic reticulum proteins that correlate with sensitivity to the toxin. Experimental Biology and Medicine. 2008;233(2):163-75.